Hearing Research 335 (2016) 149–160

Contents lists available at ScienceDirect

Hearing Research

journal homepage: www.elsevier.com/locate/heares

Research paper

Auditory steady-state responses in cochlear implant users: Effect of modulation frequency and stimulation artifacts

Robin Gransier [a, *], Hanne Deprez [a, b], Michael Hofmann [a], Marc Moonen [b], Astrid van Wieringen [a], Jan Wouters [a]

[a] ExpORL, Dept. of Neurosciences, KU Leuven, Herestraat 49 bus 721, 3000 Leuven, Belgium
[b] STADIUS, Dept. of Electrical Engineering (ESAT), KU Leuven, Kasteelpark Arenberg 10, 3001 Leuven, Belgium

ARTICLE INFO

Article history:
Received 18 November 2015
Received in revised form
4 March 2016
Accepted 14 March 2016
Available online 17 March 2016

Keywords:
Cochlear implant
Auditory steady-state response
Modulation frequency transfer function
Auditory pathway
Monopolar mode

ABSTRACT

Previous studies have shown that objective measures based on stimulation with low-rate pulse trains fail to predict the threshold levels of cochlear implant (CI) users for high-rate pulse trains, as used in clinical devices. Electrically evoked auditory steady-state responses (EASSRs) can be elicited by modulated high-rate pulse trains, and can potentially be used to objectively determine threshold levels of CI users. The responsiveness of the auditory pathway of profoundly hearing-impaired CI users to modulation frequencies is, however, not known. In the present study we investigated the responsiveness of the auditory pathway of CI users to a monopolar 500 pulses per second (pps) pulse train modulated between 1 and 100 Hz. EASSRs to forty-three modulation frequencies, elicited at the subject's maximum comfort level, were recorded by means of electroencephalography. Stimulation artifacts were removed by a linear interpolation between a pre- and post-stimulus sample (i.e., blanking). The phase delay across modulation frequencies was used to differentiate between the neural response and a possible residual stimulation artifact after blanking. Stimulation artifacts were longer than the inter-pulse interval of the 500 pps pulse train for recording electrodes ipsilateral to the CI. As a result the stimulation artifacts could not be removed by artifact removal on the bases of linear interpolation for recording electrodes ipsilateral to the CI. However, artifact-free responses could be obtained in all subjects from recording electrodes contralateral to the CI, when subject specific reference electrodes (Cz or Fpz) were used. EASSRs to modulation frequencies within the 30–50 Hz range resulted in significant responses in all subjects. Only a small number of significant responses could be obtained, during a measurement period of 5 min, that originate from the brain stem (i.e., modulation frequencies in the 80–100 Hz range). This reduced synchronized activity of brain stem responses in long-term severely-hearing impaired CI users could be an attribute of processes associated with long-term hearing impairment and/or electrical stimulation.

© 2016 Elsevier B.V. All rights reserved.

1. Introduction

Minimum and maximum electrical stimulation levels as used in cochlear implants (CI) vary across stimulation electrodes (Pfingst and Xu, 2004) and CI users (van der Beek et al., 2015). The determination of these electrode and user dependent stimulation levels can be challenging, especially for CI users who cannot give reliable behavioral feedback. Over the last decade, several methods have been studied to objectively determine the detection threshold levels (T-levels) and maximum comfort levels (C-levels) in CI users. Electrically evoked compound action potentials (ECAPs) and electrically evoked auditory brain stem responses (EABRs) have been studied extensively. ECAPs and EABRs are normally elicited with low-rate [30–80 pulses per second (pps)] pulse trains. Moderate correlations have been reported between ECAP and EABR thresholds on the one hand, and the behavioral T- and C-levels of low-rate pulse trains on the other hand (Brown et al., 2000; Hughes et al., 2000). However, methods that use low-rate pulse trains fail to predict the behavioral T-levels of high-rate (500–1200 pps) pulse trains (McKay et al., 2013; Miller et al., 2008), which are used in commercial CI devices. In general, behavioral T-levels decrease with increasing pulse rate due to temporal integration (Viemeister and

* Corresponding author.
E-mail address: robin.gransier@kuleuven.be (R. Gransier).

http://dx.doi.org/10.1016/j.heares.2016.03.006
0378-5955/© 2016 Elsevier B.V. All rights reserved.

Abbreviations

A_{sHk}	the amplitude of the harmonic k of the response
A_{sF}	the amplitude of the response at the modulation frequency
A_s	the estimated response of the synchronized to the stimulus activity
A_{s+n}	the measured response amplitude containing both synchronized and nonsynchronized to the stimulus activity
AM	amplitude modulated
ASSR	auditory steady-state response
CI	cochlear implant
C-level	maximum comfort level
C_{mod}	comfort level of the modulated pulse train
CU	current units
C_{unmod}	comfort level of the unmodulated pulse train
DC	direct current
EABR	electrically evoked auditory brain stem response
EASSR	electrically evoked auditory steady-state response
ECAP	electrically evoked compound action potential
EEG	electroencephalography
L34	research speech processor from Cochlear Ltd.
MFTF	modulation frequency transfer function
MP1+2	monopolar stimulation with both the extracochlear ball electrode and the extracochlear electrode on the casing of the receiver/stimulator as ground electrodes
NIC	Nuclues Implant Communicator from Cochlear Ltd.
$PMD_{100\%}$	100% perceptual modulation depth
POD	programming device from Cochlear Ltd.
pps	pulses per second
SNR	signal-to-noise ratio
THD_F	total harmonic distortion based on the amplitude of the fundamental frequency
THD_r	total harmonic distortion based on the root mean square value of the signal
T-level	detection threshold level
T_{unmod}	detection threshold level of the unmodulated pulse train

Wakefield, 1991). Temporal integration results in a power increase within the temporal integration period with increasing pulse rate. This power-increase is proportional to the number of pulses present within the temporal integration period. Since the T-level depends on the amount of power present within the temporal integration window, a decrease in T-level is observed with increasing pulse rate. For both acoustical and electrical stimuli, the temporal integration period is approximately 300 ms (Donaldson et al., 1997; Gerken et al., 1990; Plomp and Bauman, 1959; Shannon, 1989). The T-level decrease with increasing pulse rate, however, is highly variable across stimulation sites and ranges, on average, between −1.8 and −3 dB per doubling of pulse rate (Green et al., 2012; Kreft et al., 2004; Shannon, 1985; Skinner et al., 2000). This slope is more variable across stimulation sites for pulse rates <500 pps than for pulse rates >500 pps (McKay et al., 2013). In addition, the steepness of the slope is assumed to depend on the cochlear health, and more specifically on the survival of neural spiral ganglion cells at the stimulation site (Kang et al., 2010; Pfingst et al., 2010, 2015). This inconsistent relation between low and high pulse rate threshold levels across stimulation sites precludes objective methods that use low-rate pulse trains to determine the T-levels of high-rate pulse trains, as applied in clinical devices.

One potential alternative to objectively determine T-levels of high-rate pulse trains is the electrically evoked auditory steady-state response (EASSR). The EASSR is a stationary response that can be elicited by repetitive pulses, and by periodically varying or modulated pulse trains (Jeng et al., 2008; Hofmann and Wouters, 2012). Its acoustical counterpart [i.e., the auditory steady-state response (ASSR)] is used to objectively determine the frequency specific hearing thresholds in infants (Luts et al., 2006; Van Maanen and Stapells, 2010), and as a model to study temporal processing of speech (Liégeois-Chauvel et al., 2004; Vanvooren et al., 2014). The ASSR is the product of overall neural activity phase-locked to the stimulus (Picton et al., 2003), and, depending on the modulation frequency, originates from different regions of the auditory pathway. In subjects with normal hearing, the synchronized activity as reflected in the ASSR to modulation frequencies of 80–120 Hz predominantly originates from the upper part of the brain stem (Herdman et al., 2002; Purcell et al., 2004; Bidelman, 2015), whereas synchronized activity to modulation frequencies in the range of 30–60 Hz originates from both cortical and subcortical regions (Herdman et al., 2002; Picton et al., 2003; Purcell et al., 2004). Synchronized activity to modulation frequencies <20 Hz originates predominantly from the auditory cortices (Giraud et al., 2000; Liégeois-Chauvel et al., 2004).

The modulation frequency used to evoke the ASSR is of major importance for threshold determination. In normal hearing awake adults the most efficiently recorded ASSRs are evoked by modulation frequencies around 40 Hz (Cohen et al., 1991; Purcell et al., 2004). The 40 Hz ASSR is assumed to be the result of the superposition of transient middle latency responses (Galambos et al., 1981; Bohórquez and Özdamar, 2008) and originates from multiple generators. Auditory cortices, thalamus, and brain stem regions have been suggested as generators for the 40 Hz response (Johnson et al., 1988; Herdman et al., 2002). The 40 Hz response amplitude, however, is reduced during anesthesia and sleep (Cohen et al., 1991), and is not yet mature during the first decade of life (Levi et al., 1993; Pethe et al., 2004). Therefore, in clinical applications, where infants are tested during sleep, ASSRs that originate from the brain stem are used (80–100 Hz), since these are not affected by maturation or state of arousal (Cohen et al., 1991; Pethe et al., 2004). Currently, it is not known how the auditory pathway of long-term hearing-impaired CI users respond to different modulation frequencies. We hypothesize that the response of the auditory system to different modulation frequencies might be altered in CI users, due to degenerative processes as a consequence of their long-term profound hearing impairment, compared to normal hearing subjects. In order to use EASSRs as a fitting tool it is therefore important to gain insight into how the modulation frequency affects the EASSR in CI users.

One of the challenges when measuring EASSRs in CI users is the proper discrimination between neural response and the stimulation artifact originating from the CI. EASSR recordings are contaminated with artifacts from the RF communication link and with stimulation artifacts, which are the result of the electrical stimulation pulses. When modulating a pulse train, the stimulation artifact can have a frequency component at the modulation frequency (i.e., the response frequency). Stimulation artifacts can be removed effectively, when stimulating in bipolar mode, by interpolating over the time course of the artifact (Hofmann and Wouters, 2010, 2012). Because the duration of the stimulation

artifact under bipolar stimulation is shorter than 1 ms, pulse rates up to 1000 pps (as are used in clinical devices) can be used to measure EASSRs. However, the removal of monopolar stimulation artifacts from the electroencephalography (EEG) recording is more challenging. Compared to bipolar stimulation artifacts, monopolar stimulation artifacts are larger in magnitude (Hughes et al., 2004) and their duration is often longer than the inter-pulse interval of clinically used pulse rates. Since monopolar stimulation levels cannot be derived from bipolar stimulation levels, due to the differences in T- and C-levels across stimulation modes (Pfingst and Xu, 2004), a clinically applicable fitting method should therefore elicit EASSRs with clinically relevant pulse rates and in a monopolar stimulation mode.

In the present study we aimed to measure EASSRs, free from stimulation artifacts, with a clinical relevant pulse rate and stimulation in monopolar mode. Given that the phase characteristic of the neural response normally differs across modulation frequencies, whereas the phase characteristic of the stimulation artifact is assumed to remain constant across modulation frequencies we expected to differentiate between a neural response and an artifact dominated response based on the phase characteristic of the measured response. In addition we studied how the modulation frequency affects the EASSR in adult CI users. The results of the present study give insight in the temporal responsiveness of the electrically stimulated auditory pathway of long-term profoundly hearing-impaired CI users, and in the modulation frequencies that can be used to measure the EASSR efficiently in adult CI users.

2. Materials and methods

2.1. Subjects

Six subjects (3 male) who are under the care of the ENT Department of the University Hospital Leuven (UZ Leuven) participated in the present study. Subjects were post-lingually deaf native Flemish speakers and had more than two years' experience with their CI, with the exception of subject 4 who had only six months of experience. All subjects reported long-term profound hearing impairment prior to their CI implantation. Relevant subject details are shown in Table 1. The Medical Ethics Committee of the UZ Leuven approved this study (approval number B32220072126), and prior to participation a signed informed consent was obtained from each subject.

2.2. Stimuli & stimulus generation

Unmodulated, or amplitude modulated (AM) pulse trains were used as stimuli. All electrical pulses were symmetrical biphasic, cathodic first, pulses with a pulse width of 25 μs and an interphase gap of 8 μs. Monopolar stimulation was used. Both the extracochlear ball electrode and the extracochlear electrode on the casing of the receiver/stimulator served as the ground (MP1+2), and intracochlear electrode 11 served as the active electrode. Based on the data of a pilot study, where we estimated the duration of the stimulation artifact, we hypothesized that stimulation artifacts accompanying electrical stimulation could be removed when stimulating at a rate of 500 pps. In addition, the extrapolation from 500 pps to currently clinically used pulse rates (i.e., 900–1200 pps) results in a more reliable prediction of T-levels of high-rate pulse trains, due to the relative linear decrease of T-level with increasing pulse rate for pulse rates >500 pps, compared to predictions based on pulse rates <500 pps (McKay et al., 2013).

In order to obtain equal perceptual modulation depths across subjects; each AM pulse train was modulated in Ampere between the T-level of an unmodulated pulse train (T_{unmod}) and the C-level of the newly generated modulated pulse train (see 2.3.1 Behavioral measurements). This resulted in a 100% perceptual modulation depth ($PMD_{100\%}$) for all subjects with disregard of the intersubject variability of modulation depth in current.

All stimuli were generated with custom written software (Hofmann and Wouters, 2010) interfacing with the Nucleus Implant Communicator (NIC), and were presented to the CI through a programming device (POD) connected to a research speech processor (L34), all provided by Cochlear Ltd.

Table 1
Relevant subject details.

Subject	Age (years)	Etiology	CI experience (years)	CI device[a]
S1	54	Autoimmune	2.8	CI24RE(CA)
S2	54	Unknown	2.5	CI24RE(CA)
S3	79	Meniere	2	CI24RE(CA)
S4	44	Unknown	0.5	CI422
S5	65	Unknown	2.6	CI24RE(CA)
S6	66	Noise exposure	6	CI24RE(CA)

[a] All subjects had a Cochlear Ltd. device.

2.3. Determining the modulation frequency transfer function

The modulation frequency transfer function (MFTF) was measured from 1 to 100 Hz, in multiple sessions, and in the following order: 30–60 Hz, 70–100 Hz, 62–68 Hz, 1–28 Hz. This order allowed, in case a subject could not complete the study, to gain insight in EASSRs to modulation frequencies that can be effectively measured in normal hearing (Picton et al., 2003). A session consisted of behavioral and electrophysiological measurements. For each subject the complete MFTF was obtained within 2 or 3 sessions. Subject 6, however, could not complete the study, leaving only the results of the first session to be included.

2.3.1. Behavioral measurements

To elicit EASSRs with the same $PMD_{100\%}$ across modulation frequencies, the $PMD_{100\%}$ was determined for six modulation frequencies (i.e., 1, 10, 18, 45, 65, and 85 Hz). Stimuli lasted 1 s, except for the 1 Hz modulated stimuli which lasted 10 s. A 7-point categorical loudness scale ("inaudible", "very soft", "soft", "comfortable", "loud", "very loud", "unbearable") was used for the determination of the perceived loudness.

First, the unmodulated threshold level (T_{unmod}) was measured by presenting a 500 pps unmodulated pulse train at a starting current level of 80 CU. The level was increased with steps of 6 CU until the subject rated the perceived loudness as soft. The level was then decreased with steps of 3 CU until the stimulus was inaudible, and increased again with steps of 1 CU until the stimulus became audible again. T_{unmod} was defined as the level where the stimulus became audible again.

Second, the unmodulated comfort level (C_{unmod}) was measured with steps of 6 CU starting from T_{unmod} until the subject rated the perceived loudness of the stimulus as comfortable but loud. The level was then increased with steps of 3 CU until the subject judged the stimulus as too loud and decreased again with steps of 1 CU until the perceived loudness of the stimulus was rated as comfortable but loud. This level was defined as C_{unmod}.

Third, the modulated comfort level (C_{mod}) for each of the six modulation frequencies was determined. A pulse train was first modulated between T_{unmod} and C_{unmod}, and the maximum level was then adjusted with the same procedure as C_{unmod}. The $PMD_{100\%}$ was defined as the difference between T_{unmod} and C_{mod}.

2.3.2. Electrophysiological measurements

2.3.2.1. Stimulation. Forty-three AM pulse trains were used to measure the 1–100 Hz MFTF in each subject. The MFTF was measured with a step size of 1, 2, 3, and 3 Hz for modulation frequencies ranging from 1–10, 12–20, 30–60, and 70–100 Hz, respectively. Additionally, the modulation frequencies 22, 25, 28, 62, 65, and 68 Hz were measured to have complete coverage of the 1–100 Hz frequency range. Each AM pulse train was modulated, in Ampere, between T_{unmod} and C_{mod}. The C_{mod} of modulation frequencies not included in the behavioral measurements were set to the level of the nearest modulation frequency included in the behavioral measurements. A pilot study prior to the experiments showed no difference in perceived loudness at comfort level (i.e., C_{mod}) across modulation frequencies. Stimuli/recordings consisted of 300 epochs of 1.024 s. Modulation frequencies and pulse rates were rounded so that each epoch contained an integer number of periods and pulses. In order to synchronize stimulation and recording a trigger signal was sent at the start of each epoch from the POD to the recording setup.

2.3.2.2. Recording setup. A 64-channel Biosemi ActiveTwo EEG recording system was used for the EEG-recordings. The system, based on a direct current (DC) amplifier, had a 24 bit resolution over a 524 mV_{pp} dynamic range. A sample rate of 8192 Hz was used. EEG-signals were preamplified by Ag/AgCI active electrodes placed on the subject's head. A cap was used to position the recording electrodes according to the international standardized 10–20 system (Jasper, 1958). Recording electrodes positioned at the location of the sound processor or the coil were excluded from the EEG recordings.

Recordings were made in a soundproof and electrically shielded room. Subjects sat in a comfortable chair or laid on a bed, and were asked to move as little as possible during the recordings. In order to have the same attentional state across measurements and subjects, subjects watched a silent movie with subtitles during the measurements.

2.3.2.3. Reference electrode. The relation between the position of the CI return electrodes and the reference electrode used to measure the EASSRs may have an effect on the presence of a residual stimulation artifacts after blanking. This effect is assumed to be subject dependent, due to different head sizes, and the placement of the receiver/stimulator and ball electrode (i.e., the return electrodes). To gain insight in how the position of the reference electrode affects the presence of the residual stimulation artifact after blanking, the recordings were analyzed for two reference electrode positions. Electrode positions C_z and F_{pz} were used as reference electrodes as they are positioned in the mid-sagittal plane and differ in their anterior position relative to the cochlea (i.e., the stimulation electrode).

2.4. Analysis

2.4.1. Signal processing

All off-line signal processing was done in MATLAB. CI stimulation artifacts were removed with the blanking method (Heffer and Fallon, 2008; Hofmann and Wouters, 2010). Blanking linearly interpolates between a pre-stimulation pulse sample and a post-stimulation pulse sample. The blanking length is defined as the time between the pre-stimulation pulse sample and a post-stimulation pulse sample. In order to remove as much of the stimulation artifact as possible, the pre-stimulation pulse sample was chosen to be the sample position 100 μs before the start of the stimulation pulse, and the blanking length was set to 1900 μs. This was based on the results of the pilot study, in which we found that the measured stimulation artifacts, when stimulating in MP1+2 mode, had an average length below 1.5 ms and around 2 ms for the contralateral and ipsilateral recording electrodes, respectively. After blanking, signals were high-pass filtered with a 2nd order Butterworth high-pass filter with a cut-off frequency of 2 Hz to remove any DC component in the recordings. The recordings were, based on the triggers, divided into 300 epochs with a length of 1.024 s, each resulting in a duration of approximately 5 min per recording. 5% of the epochs were removed from the recording, based on the highest peak-to-peak amplitudes, as they were assumed to contain muscle and other recording artifacts.

The complex frequency spectrum was calculated for each epoch separately by means of a Fast Fourier Transform, with a frequency resolution of 0.97 Hz, and the complex frequency spectrum of the reference electrode was subtracted from the complex frequency spectrum of each recording electrode. The inverse gain of the high-pass filter was applied to the frequency spectrum of each epoch to compensate for the filter effects on the magnitude of the response. For each epoch the response amplitudes and phases, at the response spectrum, were obtained from the complex frequency spectrum corresponding to the modulation frequency or its harmonics (i.e., the response spectrum). Mean response amplitudes and phases were computed by vector averaging over epochs. The one-sample Hotelling T^2 (Hotelling, 1931) was used, for each recording electrode, to determine if the synchronized activity (i.e., measured response) differed significantly from the non-synchronized activity (i.e., neural background activity). This test compares the average real and imaginary component of the response bin against the variability across epochs of the same response bin. A significance level of 5% was applied. The amplitude of the neural background activity in the response bin at the response frequency was calculated as the standard deviation over all epochs divided by the square-root of the number of epochs.

2.4.2. Residual stimulation artifacts and MFTF analysis

For each recording electrode the presence of residual stimulation artifacts, after blanking, was assessed based on the phase delay (Picton et al., 2003). The phase delay was calculated by 'unwrapping' the absolute phase across modulation frequencies, so that the phase at each modulation frequency was within 180° the phase of its neighboring modulation frequencies. For normal hearing subjects, the ASSR phase delay increases with increasing modulation frequency (Stapells et al., 1987; Cohen et al., 1991; Picton et al., 1987). Artifact dominated recordings, however, result in significant responses with a constant phase delay across modulation frequencies, at a multiple of 180° (Hofmann and Wouters, 2012). Per subject, the recording electrodes with artifact-free responses located in parietal-temporal and occipital regions were included in the analysis of the MFTF (see Fig. 2 for the position of the recording electrodes on the scalp). Recording electrodes in the parietal-temporal and occipital regions were considered artifact-free if the phase delay of the significant responses increased with increasing modulation frequency and contained no region that had a constant phase delay at an integer multiple of 180°. Per hemisphere, the average amplitude of the response and the neural background activity was calculated based on the average power sum across electrodes, whereas the linear signal-to-noise ratio (SNR) was averaged across electrodes and converted to a dB value.

To obtain a generic insight in the modulation frequency regions that are more or less responsive, the MFTF was divided into different oscillatory bands: δ (1–3 Hz), θ (4–7 Hz), α (8–12 Hz), β (13–20 Hz), and γ (22–100 Hz) band.

To gain insight in the harmonic content of the evoked activity, the response bins at the modulation frequency and its first five harmonics were analyzed. A harmonic frequency is defined as

$H_k = (1 + k)F$, where F is the modulation frequency and k number of the harmonic. The total harmonic distortion (THD_F) was calculated, as the harmonic content of the signal (i.e., the power sum of the first five harmonics) compared to the amplitude of the modulation frequency [equation (1)]. This way of analyzing the THD_F was chosen in favor of the harmonic sum or THD_r, where the denominator in equation (1) is replaced with the root-mean-square value of the signal. The THD_F gives a better insight in the power at the harmonic frequency, especially if the power at the harmonic frequency is higher than the power at the modulation frequency (Shmilovitz, 2005). Because the artifact removal procedure acts as a down sampling of the signal, the THD_F was only calculated for modulation frequencies up to 40 Hz. To minimize the effect of the neural background activity, which follows a 1/f distribution, the unbiased response amplitude [equation (2)] was used to calculate the THD_F, i.e.:

$$THD_F = \frac{\sqrt{A_{s\,H1}^2 + A_{s\,H2}^2 + \ldots + A_{s\,Hk}^2}}{A_{s\,F}} \quad (1)$$

Where $A_{s\ Hk}$ is the unbiased response amplitude at the k^{th} harmonic [$H_k = (1 + k)F$], and $A_{s\ F}$ is the unbiased response amplitude at the modulation frequency.

$$A_s = \sqrt{A_{s+n}^2 - A_n^2} \quad (2)$$

A_{s+n} is the measured amplitude (containing both response and neural background activity), A_n is the amplitude of the neural background activity, and A_s is the estimated response amplitude of the synchronized activity. Negative unbiased response amplitudes were set to zero.

Latencies for the frequency regions 2–20 Hz, 30–50 Hz, and 80–100 Hz were calculated per recording electrode by dividing the slope of the phase delay, based on a linear fit of the phase delay of the significant responses, by 360° [i.e., the apparent latency (Regan, 1966; Picton et al., 2003)]. Apparent latencies were only calculated if a recording electrode contained three or more significant responses within a frequency region.

2.4.3. Statistical analysis

All statistical analyses were preformed in MATLAB. Due to the lack of normality and the relatively small sample size, for both the behavioral and the electrophysiological data, all analyses were carried out with nonparametric tests. Unless indicated otherwise, a significance level of 5% was applied.

3. Results

3.1. Behavioral measurements

Unmodulated behavioral thresholds varied between 107 and 163 CU, and 140 and 193 CU for T_{unmod} and C_{unmod}, respectively. Wilcoxon signed-rank test showed no significant difference between the first and the last session for both T_{unmod} ($T = 4$, $p = 1$) and C_{unmod} ($T = 13.5$, $p = 0.1875$). Fig. 1 shows the C_{mod} and the $PMD_{100\%}$ for each subject and modulation frequency. Friedman's ANOVA showed that neither the C_{mod} ($\chi^2(5) = 10.58$, $p = 0.0603$) nor the $PMD_{100\%}$ ($\chi^2(5) = 9.02$, $p = 0.1082$) differed significantly across modulation frequencies. The C_{mod} was on average 9 CU (range: 0–16 CU) higher than the C_{unmod}, and the average $PMD_{100\%}$ across modulation frequencies and subjects was 44 CU (range: 20–88 CU).

3.2. Presence of stimulation artifacts

Fig. 2 shows the phase delay for each recording electrode for two representative subjects. In case no artifact removal was applied and when stimulation artifacts dominated the neural responses, a constant phase delay was observed at an integer multiple of 180°, at all recording electrodes and across all modulation frequencies that had responses that differed significantly (based on the one-sample Hotelling T^2 test, $p < 0.05$) from the neural background noise (Fig. 2A). If the neural response magnitude was larger than the stimulation artifacts, an increasing phase delay was observed for the modulation frequency regions where the neural response dominated the recording. The phase delay, however, becomes constant at an integer multiple of 180° when the neural response magnitude decreases to a level well below the magnitude of the stimulation artifact (i.e., a stimulation artifact dominated response). This is shown in Fig. 2C where an increasing phase delay is observed for modulation frequencies <50 Hz and a constant phase delay for modulation frequencies >50 Hz, although these responses differed significantly from the neural background noise.

Stimulation artifacts could not be removed from ipsilateral recording electrodes when blanking was applied. Responses recorded with ipsilateral recording electrodes differed significantly from the neural background activity for all modulation frequencies, and had a constant phase delay at an integer multiple of 180°. At contralateral recording electrodes, however, the stimulation

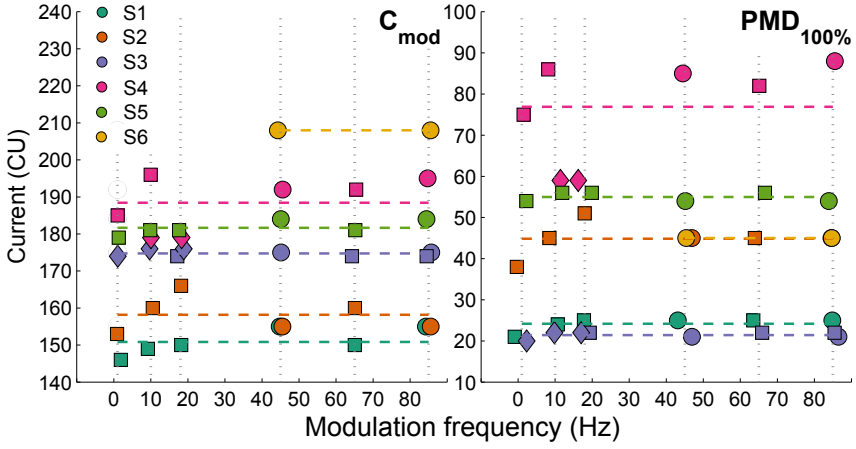


Fig. 1. The modulated C-levels (C_{mod}) and the 100% perceptual modulation depth ($PMD_{100\%}$) per subject obtained during the first (○), second (□), and third session (◇). Dashed lines indicate, per subject, the average across modulation frequencies and sessions.

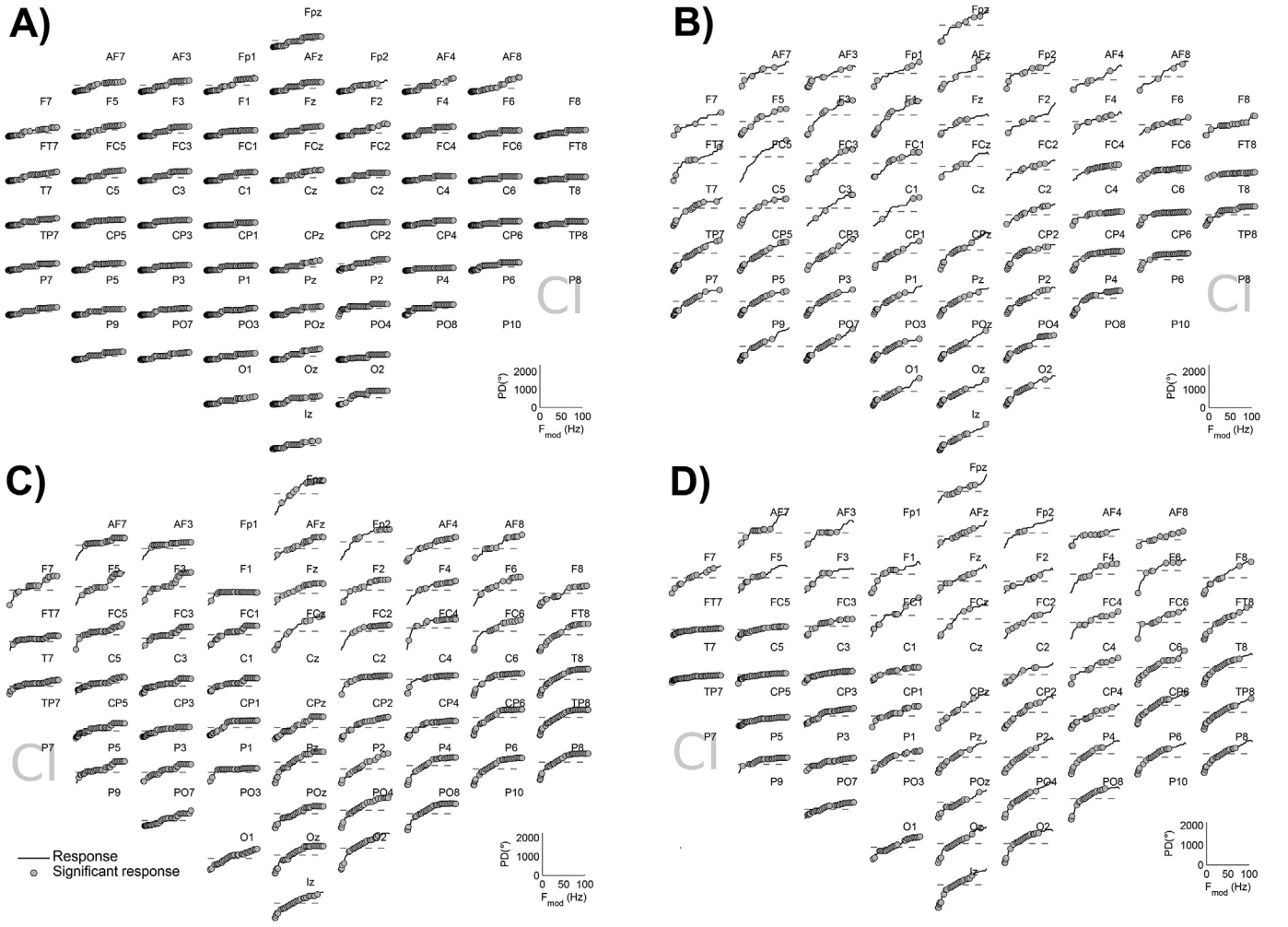


Fig. 2. The phase delays (PD) as a function of the modulation frequency (F_{mod}) of all recording electrodes for two representative subjects: S2 and S3. Figure A(S2) and C(S3) show the phase delays of the recorded responses when artifact removal was not applied. Figure B(S2) and D(S3) show the phase delays after artifact removal has been applied. Cz is used in both examples as a reference. The cochlear implant of subject S2 and S3 is located on the right and left hemispheres, respectively. Recording electrodes positioned at the coil were for S2: TP8, P6, P8, P10, and PO8 and for S3: P7 and P9. Recording electrode P10 and PO3 of S3 were removed from the analysis due to a poor connection in one of the sessions. The horizontal dashed lines indicate the closest to the median phase delay integer multiple of 180° (i.e., the expected phase of the stimulation artifact). Responses that significantly differed from the neural background activity are marked (●).

artifacts could be removed. The phase delay of the significant responses, at contralateral electrodes, increased with increasing modulation frequency. In addition, no significant responses were detected for modulation frequencies within the 80–100 Hz range, indicating that blanking reduced the stimulation artifact to a level where it did not significantly differ from the background activity (Fig. 2B and D).

Wilcoxon rank-sum tests indicated that the phase delay slopes (20–100 Hz) of the contralateral recording electrodes were significantly higher than the phase delay slopes of the ispilateral recording electrodes for both reference electrodes: Cz ($W_s = 3563$, $p < 0.001$) and Fpz ($W_s = 3190$, $p < 0.001$). There was a significant effect of subject on the difference in the phase delay slope between reference electrodes for the contralateral recording electrodes, $\chi^2(5) = 27$, $p < 0.001$. Post hoc analysis, based on Wilcoxon signed-rank tests, showed significantly higher phase delay slopes for the Fpz reference electrode compared to Cz for subject S4 ($T = 6$, $p = 0.0013$) and S5 ($T = 1$, $p < 0.001$).

Per subject, artifact-free recording electrodes were selected based on the individual phase delays of each electrode. In case there was no significant difference between reference electrodes, Cz was used as reference electrode. Fpz was used as reference electrode for subject S4 and S5, as the phase delay slope was significantly higher for this reference electrode than for Cz. For all subjects, stimulation artifacts were still present at ipsilateral recording electrodes. Therefore the artifact-free recording electrode selection was only based on contralateral recording electrodes. The contralateral recording electrode selection, was based on the a priori electrode selection for all subjects, except for subject S4. A portion of the a priori selected electrodes of S4 contained artifact dominated responses. These electrodes had significant responses with a constant phase delay in the 80–100 Hz region. Based on the phase delay curves of the individual electrodes, an artifact-free selection of recording electrodes was made. The selected artifact-free electrodes of all subjects and the corresponding phase delays are shown in Fig. 3.

3.3. Modulation frequency transfer function

3.3.1. Modulation frequency

Fig. 4 shows the individual MFTFs of all subjects derived from the artifact-free recording electrodes. The δ band (1–4 Hz)

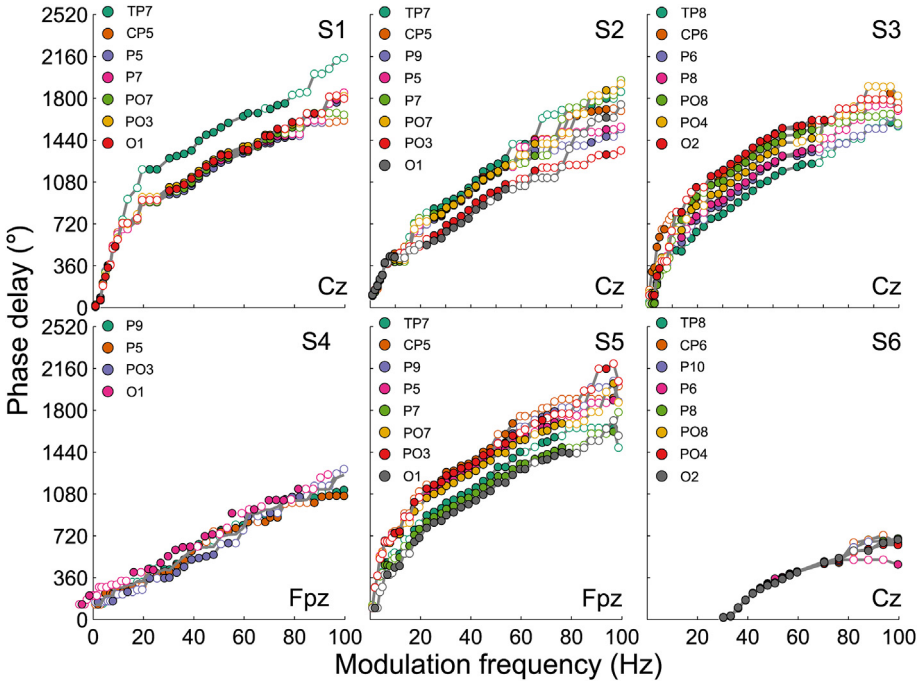


Fig. 3. For each subject, the phase delay of the artifact-free recording electrodes located in the parietal-temporal and occipital regions of the hemisphere contralateral to the CI is shown. Reference electrode Cz was used for all subjects, except for S4 and S5, where Fpz was used as the reference electrode. Recording electrode P9, and P10 of respectively subject S1 and S3 were removed from the analysis due to a poor connection in one of the sessions. Responses that significantly differed from the neural background activity are represented by the filled circles.

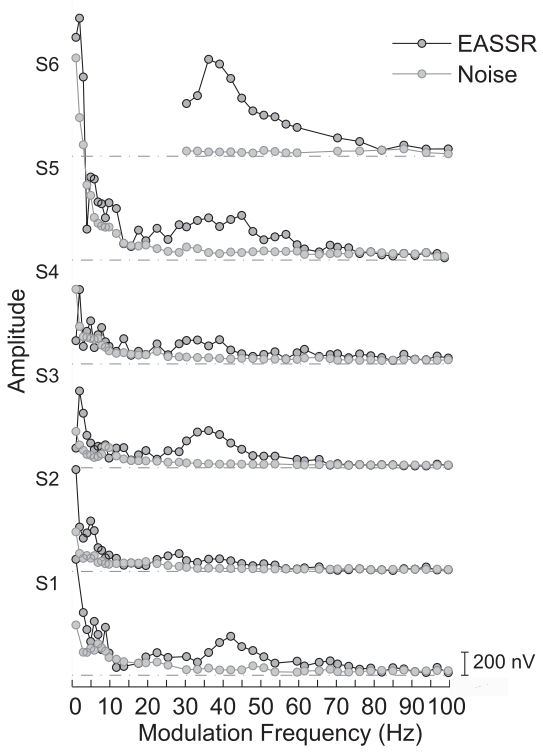


Fig. 4. The individual modulation frequency transfer functions. Response and neural background activity amplitudes are based on the average power across artifact-free electrodes (see Fig. 3). Light gray filled circles indicate the neural background activity and dark gray filled circles represent the EASSR measured at the modulation frequency. Subject 6 participated only in the first session, therefore not all modulation frequencies were tested.

contained the most prominent responses of the cortical evoked EASSRs (1–20 Hz). Of the five subjects who completed all conditions in the study only S5 did not have significant responses within this band. Across the subjects who completed all conditions of the study only 6, 5, and 4 significant responses were found to modulation frequencies within the θ (4–7 Hz), α (8–12 Hz), and β (13–20 Hz) range, respectively. The most prominent responses, across all modulation frequencies, were located in the 30–50 Hz γ range, with a clear peak at 40 Hz (see also Figs. 5 and 6). All subjects had a significant response at 40 Hz and the average SNR and amplitude at this frequency is 16.9 dB (range = 12.2–26.9 dB) and 326.8 nV (range = 109.9–799.5 nV), respectively. Only two subjects (S4 and S6) had significant responses, averaged across the artifact-free recording electrodes, within the 80–100 Hz γ range.

Biedelman (2015) reported optimal differential electrodes configurations to measure brain stem responses where Fpz and electrodes placed at the mastoid. In order to ensure that the small number of observed brain stem responses were not due to averaging across electrodes and the use of Cz as a reference we analyzed the modulation frequencies within the 80–100 Hz γ range for all artifact-free electrodes and for both reference electrodes. Neither the recording electrode position nor the reference electrode position had an effect on the number of significant responses measured within the 80–100 Hz range.

3.3.2. Harmonics

Fig. 6 shows the group average MFTF for the different components of the response. In accordance with the data of normal hearing subjects (Ross et al., 2000), harmonic frequencies that were within the 30–50 Hz region had higher amplitudes compared to their modulation frequency (i.e., modulation frequencies <25 Hz). As can be derived from the THD_F (Fig. 7), modulation frequencies within the 12–20 Hz range resulted in EASSRs with dominant components at the first harmonic, even in the absence of a

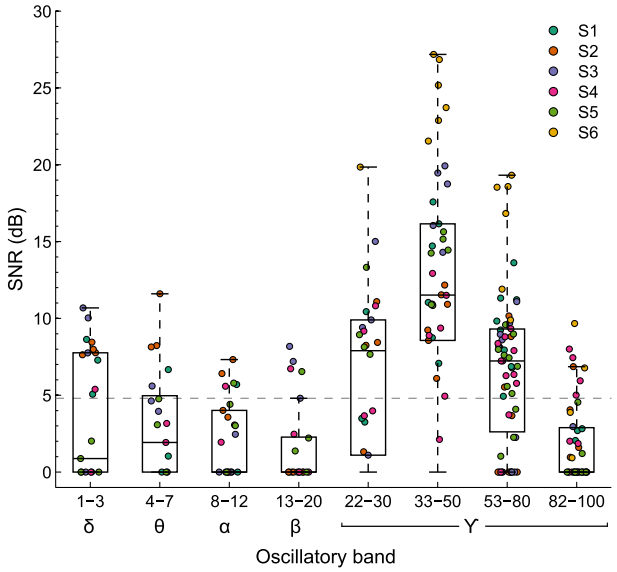


Fig. 5. Per oscillatory band: δ (1–3 Hz), θ (4–7 Hz), α (8–12 Hz), β (13–20 Hz), and γ band (22–100 Hz) the subject dependent averaged responses across artifact-free recording electrodes (see Fig. 3) are shown. The γ band was divided into four unique modulation frequency regions to visualize the differences in responsiveness between the different γ regions. The dashed line represents the SNR that corresponds to a significance level of 5%. Individual data points are color coded and jittered along the horizontal axis within each oscillatory band to aid readability.

significant response component at the modulation frequency. The response magnitude at the modulation frequency was in all subjects predominant over the response magnitude at the harmonic frequencies for modulation frequencies >30 Hz.

3.3.3. *Apparent latencies*

Fig. 8 shows the apparent latencies across subjects for different modulation frequency regions. Median apparent latencies (and interquartile ranges) of all recording electrodes were 106.5 (63.4), 44.2 (6.8), and 15.3 (18.6) ms for the 2–20, 30–50, and 80–100 Hz regions, respectively. Wilcoxon rank-sum tests indicated that the apparent latencies across subjects (i.e., per subject the apparent latencies across recording electrodes were averaged) of the 2–20 Hz region (Mdn = 106.5 ms) were significantly larger than

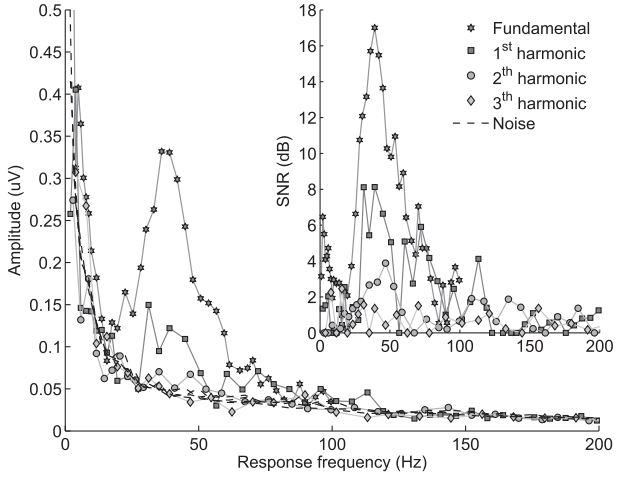


Fig. 6. Group average per response frequency in terms of amplitude and SNR for the fundamental frequency (i.e., the modulation frequency), and its 1st, 2nd, and 3rd harmonic.

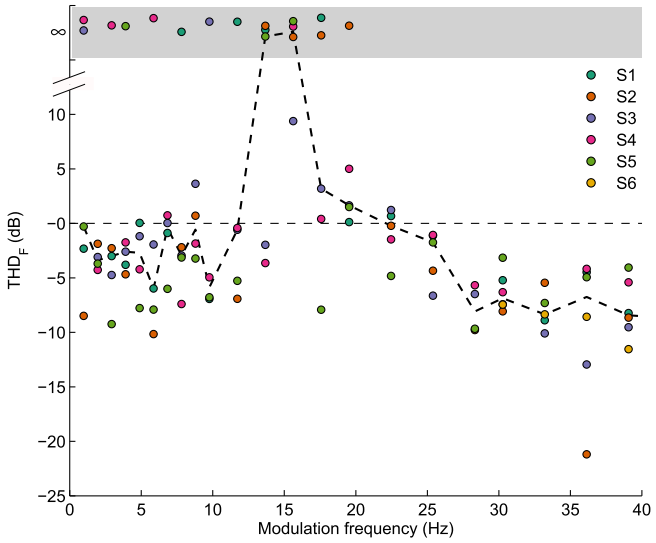


Fig. 7. The THD_F based on the first five harmonics per subject for modulation frequencies up to 40 Hz. To aid readability jitter was applied to THD_F values that were infinite. The dashed black line shows the median across subjects. A positive THD_F means that there was more power present at the harmonics compared to the modulation frequency, and vise versa for a negative THD_F.

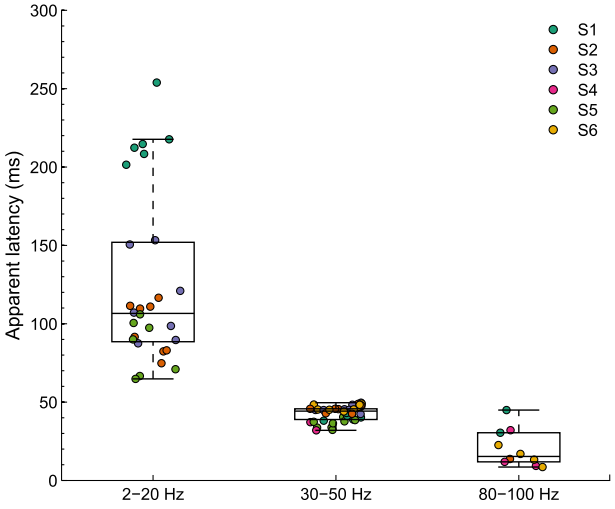


Fig. 8. Apparent latencies of the artifact-free recording electrodes (see Fig. 3) of each subject for the modulation frequency regions 2–20, 30–50, and 80–100 Hz. Different colors indicate the apparent latencies derived from the recording electrodes of a specific subject. Individual data points are jittered along the horizontal axis to aid readability.

the apparent latencies of the 30–50 Hz region (Mdn = 44.2 ms) $W_s = 34$, $p < 0.01$, and the 80–100 Hz region (Mdn = 15.3 ms), $W_s = 26$, $p = 0.029$. Apparent latencies of the 30–50 Hz region were significantly larger than those of the 80–100 Hz region, $W_s = 44$, $p = 0.019$.

4. Discussion

Research aimed at the objective determination of T-levels (e.g., Mckay et al., 2013) indicates that T-levels of clinically used pulse rates cannot be predicted reliably based on low pulse rate measures (i.e., <100 pps). This has resulted in a need for an objective method that can measure T-levels with clinically relevant pulse rates. Hofmann and Wouters (2012) showed that EASSRs can be used to

objectively measure T-levels with clinically relevant pulse rates when stimulating in a bipolar mode. Measuring EASSRs when stimulating in the clinically used, monopolar mode, and with clinically relevant pulse rates remains, however, challenging. Since monopolar stimulation artifacts are higher in magnitude and longer in duration they are more difficult to attenuate or remove from the recording. In the present study we were able to remove the monopolar stimulation artifact and record EASSRs from the recording electrodes contralateral to the CI. Results show a different responsiveness across modulation frequencies within the 1–100 Hz range. The results of the present study deviate from those of normal hearing subjects reported in literature, especially for modulation frequencies within the 80–100 Hz γ range.

4.1. Modulation frequency and perceived loudness

To ensure that the stimulation level across modulation frequencies did not affect the modulation frequency specific EASSR, we investigated the C_{mod} across modulation frequencies. No significant group level differences were found across modulation frequencies for C_{mod}. This indicates that there is no direct causality between the differences in evoked responses across modulation frequencies and the current levels used. The results of the present study are in line with the assumption and results of McKay and Henshall (2010). They reported, based on the predictions of the McKay and McDermott (1998) loudness model, that there is no effect of modulation frequency on the perceived loudness as long as the cycle of the modulation is shorter than the temporal integration window (i.e., 2–4 ms). However, if the duration of a modulation cycle exceeds the temporal integration window, the model output will fluctuate and the model cannot predict the perceived loudness. Results of the present study, where equal current resulted in equal comfort levels across modulation frequencies, can be explained by adding the multiple-look model of Viemeister and Wakefield (1991) to the McKay and McDermott (1998) loudness model. After the initial temporal integrator (2–4 ms), a multiple-look integrator (300 ms) will determine the perceived loudness. As a result, and as suggested by McKay and Henshall (2010), modulation frequencies <250 Hz stimulated with equal current levels result in equal loudness.

Subject S4 had lower C_{mod} levels for the 10 and 20 Hz modulation frequencies during session three than for the other modulation frequencies measured during session one and two. This difference was not related to the modulation frequency, but presumably to a session effect. At the time of the first and second session S4 had only 6–8 months of experience whereas at session three S4 had approximately twelve months of experience. S4 also reported reduced C-levels over the six months time course between these sessions.

4.2. Effect of the stimulation artifact on the EASSR

With the blanking method we were able to remove monopolar mode stimulation artifacts of a 500 pps modulated pulse train for recording electrodes contralateral to the CI. Results show that the phase delay across modulation frequencies gives valuable information for the distinction between a neural response and residual stimulation artifact after blanking. Unlike the ASSR and the EASSR which both have a monotonically increasing phase delay across modulation frequencies (Stapells et al., 1987; Cohen et al., 1991; Picton et al., 1987), the phase of the stimulation artifact is nearly independent of the modulation frequency, since it only depends on the initial phase of the stimulus and has in absence of a neural response a constant phase delay at a multiple integer of 180°.

To determine if blanking completely removed the stimulation artifact from the recording or that a residual stimulation artifact has no influence on the measured neural response, the following factors need to be taken into account: First, the level of the neural background activity, which has a $1/f$ distribution, whereas the stimulation artifact amplitude is constant across modulation frequencies. A residual stimulation artifact, therefore, can result in a significant response at higher modulation frequencies (i.e., lower neural background activity levels) whereas this is not the case for lower modulation frequencies (i.e., higher neural background activity levels). Second, the interaction between the current level used to evoke the response and the evoked response determines if a residual stimulation artifact is problematic. Both the magnitude of the stimulation artifact and that of the EASSR depend on the current level used for stimulation (Hofmann and Wouters, 2010, 2012). In case the EASSR is larger than the residual artifact, there will be little influence of the residual stimulation artifact on the measured response. However, if the amplitude of the EASSRs is small [e.g., at high modulation frequencies (>70 Hz), less responsive modulation frequencies, or at low intensities] the stimulation artifact will be dominating the measured response (e.g., see Fig. 2C). For recording electrodes contralateral to the CI only a small number of significant responses were found for modulation frequencies within the 80–100 Hz range. Responses that were significantly different from the neural background activity had apparent latencies that were comparable with those of normal hearing subjects (see Picton et al., 2003). Taking the above into account, one can conclude that for the selected recording electrodes the stimulation artifact was completely removed, or at least reduced to a level below the lowest background level measured. However, at recording electrodes ipsilateral to the CI the stimulation artifact could not be removed (i.e., its duration was longer than the 1900 μs blanking length).

Results indicate that, for stimulation in monopolar mode, the artifact duration at the ipsilateral side is longer than the interpulse interval of the 500 pps pulse train (i.e., 2 ms). There is a high probability that, in case the CI return electrode is in close proximity of the reference electrode, the stimulation artifact present at the reference electrode has a duration that exceeds the blanking length. As a result of subtraction the stimulation artifact will then be present at all recording electrodes. By choosing a more frontal located reference electrode (Fpz in the present study) this problem can be overcome, as was the case for subject S5, and for the recording electrodes with the same artifact characteristics as the reference electrode for subject S4.

Even though more sophisticated artifact removal methods need to be developed to remove the stimulation artifact from all recording electrodes, and in order to get insight in hemispheric specific processing of modulation frequencies, the present study shows that EASSRs can be measured reliably when stimulating in monopolar mode and with clinically relevant pulse rates. Therefore, and in contrast to ECAPs and EABRs which unreliably predicts the T-levels of high-rate pulse trains (McKay et al., 2013), EASSRs could possibly be a promising objective method for the determination of T-levels of high-rate pulse trains as used in clinical devices.

4.3. How the modulation frequency affects the EASSR

Most MFTF studies in normal hearing subjects used rather large frequency step sizes to measure the transfer function (e.g., Cohen et al., 1991; Levi et al., 1993; Dobie and Wilson, 1998). In the present study, the relative small frequency step sizes used resulted in a detailed insight in how the modulation frequency affects the EASSR of long-term hearing-impaired CI users. One of the factors to take into account when interpreting the results of the present study is the recording duration. For each modulation frequency a fixed recording duration of 5.12 min was used. Since the detection of a

significant response depends both on the level of the response and of the neural background activity, and given that level of the neural background activity theoretically decreases with $1/\sqrt{n}$, the determination of a significant response for equal in magnitude responses is mainly determined by the $1/f$ distribution of the neural background activity across modulation frequencies. Therefore, the absence of a significant response, especially to modulation frequencies <20 Hz, should not be taken as an indication that there is no response present at these frequencies, it can only, not be differentiated from the background activity given the recording time of 5.12 min.

Responses to modulation frequencies <20 Hz predominately originate from the auditory cortex (Giraud et al., 2000; Liégeois-Chauvel et al., 2004). Although, a detailed study of the ASSR transfer function for modulation frequencies <20 Hz is lacking in the literature, several studies investigated synchronized activity to low modulation frequencies in the context of temporal processing in normal hearing. Wang et al. (2012) reported that the MFTF of low modulation frequencies generally follows a low-pass pattern. These results are in line with Alaerts et al. (2009) and Tlumak et al. (2011). In addition Alaerts et al. (2009) found increased amplitudes and better SNRs at 4, 10, and 20 Hz. This low pass pattern is also observed at group level in the present study. However, at individual level (Fig. 4) there is a trend that different subjects are more, or less responsive to specific modulation frequencies within the 0–20 Hz region. This suggests an intersubject variability in cortical response patterns. The average apparent latency of the cortical generated EASSRs (124.8 ms) are comparable to the 117 ms latency reported by Alaerts et al. (2009). N1 and P2 responses occur at approximately the same time scale as low modulation frequency EASSRs, and originate from the planum temporale and Heschl's gyrus, respectively (Lütkenhöner and Steinsträter, 1998). It is therefore assumed that the main generator(s) of the EASSRs to modulation frequencies <20 Hz are located within the auditory cortices. In contrast to the data of Tlumak et al. (2011) who used short tone burst to elicit cortical responses, we did not find a rich harmonic content in the EASSR for these low modulation frequencies. The lack of harmonic content for low modulation frequencies may be explained by the non-transient characteristics of the stimulus in the present study, compared to the transient stimulus used by Tlumak et al. (2011).

EASSRs within the 40 Hz region had the highest amplitude and SNR for both the modulation frequency and the harmonics. As indicated by the THD_F (Fig. 7) this response was even present for harmonics of modulation frequencies that did not have any significant response at the modulation frequency. This is comparable with the literature on ASSRs elicited in normal hearing subjects (Cohen et al., 1991; Dobie and Wilson, 1998; Poulsen et al., 2007; Ross et al., 2000). Acoustically evoked 40 Hz responses originate from multiple generators including the brain stem, thalamus and auditory cortices (Johnson et al., 1988; Herdman et al., 2002) and have average apparent latencies of 39.8 ms (Picton et al., 1987). Based on the average apparent latency of the 30–50 Hz region of the present study and the 41.5 ms average latencies reported by Hofmann and Wouters (2012), it is assumed that the origin of the 40 Hz EASSR in CI users involves similar anatomical regions as the 40 Hz ASSR in normal hearing subjects.

40 Hz ASSR amplitudes in normal hearing subjects are approximately 200–400 nV (Picton et al., 2003). EASSR amplitudes found in the present study are in line with these results, except for the high EASSR amplitudes of S6. High 40 Hz EASSR amplitudes were also found by Luke et al. (2015). They reported one CI subject with 600 nV amplitude 40 Hz responses. A possible explanation is related to direct electrical stimulation of the auditory nerve. In contrast to acoustic stimulation where the firing of neurons is related to the basilar membrane displacement, which has different time delays for different tonotopic regions, electrical stimulation simultaneously activates the neurons allocated to different tonopical locations. When these time delays are compensated higher ASSR amplitudes can be obtained. Elberling et al. (2007), for example, used acoustical chirp stimuli to increase the temporal synchronization of neural elements across different tonotopical regions in the cochlea of normal hearing subjects, and reported that ASSR amplitudes increased by a factor of 2–2.5 when using stimuli that compensated for the basilar membrane delay compared to standard click stimuli.

Even though, electrical stimulation results in a high temporal synchronization across tonotopically organized neural populations, only a limited number of responses within the 80–100 Hz γ region were significantly different from the neural background activity. These results are in contrast with the perception of modulation frequencies within this range. Psychophysical assessment of the MFTF shows that CI users have a good modulation perception up to 150 Hz (Fraser and McKay, 2012). The discrepancy between the EASSR MFTF and the psychophysical MFTF can be accounted for by the different regions of the auditory pathway involved in the two metrics. EASSRs to different modulation frequencies originate from rather distinct regions of the auditory pathway, whereas the perception of the different modulation frequencies involves the whole auditory pathway and other parts of the cortex. Absence of an electrophysiological response does, in this content therefore, not mean that the stimulus and its modulation are not perceived. In normal hearing subjects 80–100 Hz ASSRs originate predominately from the upper part of the brain stem (Herdman et al., 2002; Bidelman, 2015), and more specifically from the inferior colliculus (Bidelman, 2015). While 80–100 Hz ASSR can be measured effectively in normal hearing subjects, they have reduced magnitudes with advancing age (Picton et al., 2005). In addition, auditory deprivation could be a contributing factor to the absence of these phase-locked brain stem responses in CI users. Animal studies show that both long-term deafness as well as chronic electrical stimulation of the deafened auditory pathway alters the temporal resolution of the inferior colliculus (e.g., Vollmer et al., 2005). This suggests that the responsiveness of the brain stem to 80–100 Hz modulation frequencies of long-term hearing-impaired adults CI users differs from the responsiveness of the normally developed brain stem of normal hearing subjects.

In order to use EASSRs as a clinical tool for the objective fitting of T-levels in awake adult CI users, modulation frequencies within the 30–50 Hz γ range should be considered, as these can be measured effectively. However, how these results can be transferred to children and infants with a CI is not yet known. Responses in the 40 Hz region are affected by maturation and state of arousal (Cohen et al., 1991; Pethe et al., 2004), and are therefore, and in contrast to 80–100 Hz ASSRs, not used for hearing threshold determination. Mühler et al. (2014), however, showed that 40 Hz ASSRs can also be measured in sedated infants when narrow-band chirps are used to obtain a good temporal synchronization of neural elements, and that the resulting response magnitudes do not differ from 80–100 Hz ASSRs. In pursuit of an objective method for clinically used pulse rates, and given the differences in responsiveness to modulation frequencies over the time course of maturation, future research should investigate which modulation frequencies can be used to measure EASSRs effectively, independent of state of arousal, in both children and infants with a CI.

5. Conclusion

The present study investigated if EASSRs, when stimulating with a clinically relevant pulse rate and in monopolar mode, can potentially be used for the objective determination of high pulse

rate T-levels. Results show that, at a pulse rate of 500 pps, monopolar stimulation artifacts can effectively be removed with the blanking method at recording scalp electrodes contralateral to the CI. Neural responses could effectively be differentiated from artifact dominated responses by means of the phase information across modulation frequencies. Results show that, for 5.12 min recordings, EASSRs are most prominent and can be elicited in all subjects, within the 30–50 Hz γ region. A clear peak was observed at 40 Hz. In contrast to ASSRs in normal hearing subjects, 80–100 Hz γ range responses could not be effectively measured in adult CI users. Therefore, the 30–50 Hz range of modulation frequencies should be considered for the objective fitting of T-levels in adult CI users.

Acknowledgments

Authors would like to thank all subjects who participated in the study. Maaike Van Eeckhoutte and Robert Luke are acknowledged for their assistance during the data collection. Tom Francart is acknowledged for his valuable feedback throughout the study. Two anonymous reviewers are thanked for their valuable comments on an earlier version of the manuscript. Research was funded by a research grant (G.066213) of the Research Foundation Flanders (FWO), and a research grant (110722) and a Ph.D. grant (141243) to R. Gransier by the Flemish Agency for Innovation by Science and Technology (IWT).

References

Alaerts, J., Luts, H., Hofmann, M., Wouters, J., 2009. Cortical auditory steady-state responses to low modulation rates. Int. J. Audiol. 48, 582–593.
Bidelman, G.M., 2015. Multichannel recordings of the human brainstem frequency-following response: scalp topography source generators, and distinctions from transient ABR. Hear. Res. 323, 68–80.
Bohórquez, J., Özdamar, Ö., 2008. Generation of the 40Hz auditory steady-state response (ASSR) explained using convolution. Clin. Neurophysiol. 119, 2598–2607.
Brown, C.J., Hughes, M.L., Luk, B., Abbas, P.J., Wolaver, A., Gervais, J., 2000. The relationship between EAP and EABR thresholds and levels used to program the Nuclues 24 speech processor: data from adults. Ear Hear. 21, 151–163.
Cohen, L.T., Rickards, F.W., Clark, M.C., 1991. A comparison of steady-state evoked potentials to modulated tones in awake and sleeping humans. J. Acoust. Soc. Am. 90, 2467–2479.
Dobie, R.A., Wilson, M.J., 1998. Low-level steady-state auditory evoked potentials: effects of rate and sedation on detectability. J. Acoust. Soc. Am. 104, 3482–3488.
Donaldson, G.S., Viemeister, N.F., Nelson, D.A., 1997. Psychometric functions and temporal integration in electric hearing. J. Acoust. Soc. Am. 101, 370–3721.
Elberling, C., Don, M., Cebulla, M., Strüzebecher, 2007. Auditory steady-state responses to chirp stimuli based on cochlear traveling wave delay. J. Acoust. Soc. Am. 122, 2772–2785.
Fraser, M., McKay, C.M., 2012. Temporal modulation transfer functions in cochlear implantees using a method that limits overall loudness cues. Hear. Res. 283, 59–69.
Galambos, R., Makeig, S., adn Talmachoff, R.J., 1981. A 40-Hz auditory potential recorded from the human scalp. Proc. Natl. Acad. Sci. 75, 2643–2647.
Gerken, G.M., Bhat, V.K.H., Hutchison-Clutter, M., 1990. Auditory temporal integration and the power function model. J. Acoust. Soc. Am. 88, 767–778.
Giraud, A., Lorenzi, C., Ashburner, H., Wable, J., Johnsrude, I., Frackowiak, R., Kleinschmidt, A., 2000. Representation of the temporal envelope of sounds in the human brain. J. Neurophysiol. 84, 1588–1598.
Green, T., Faulkner, A., Rosen, S., 2012. Variations in carrier pulse rate and the perception of amplitude modulation in cochlear implant users. Ear Hear. 33, 221–230.
Heffer, J.F., Fallon, J.B., 2008. A novel stimulus artifact removal technique for high-rate electrical stimulation. J. Neurosci. Meth. 170, 277–284.
Herdman, A.T., Lins, O., Van Roon, P., Stapells, D.R., Scherg, M., Picton, T.W., 2002. Intracerebral sources of human auditory steady-state responses. Brain Topogr. 15, 69–86.
Hofmann, M., Wouters, J., 2010. Electrically evoked auditory steady state responses in cochlear implant users. J. Assoc. Res. Otolaryngol. 11, 267–282.
Hofmann, M., Wouters, J., 2012. Improved electrically evoked auditory steady state response thresholds in humans. J. Assoc. Res. Otolaryngol. 13, 573–589.
Hotelling, H., 1931. The generalization of the student's ratio. Ann. Math. Stat. 2, 360–378.
Hughes, M.L., Brown, C.L., Abbas, P.J., Wolaver, A.A., Gervais, J.P., 2000. Comparison of EAP thresholds with MAP levels in the Nucleus 24 cochlear implant: data from children. Ear Hear. 21, 164–174.
Hughes, M.L., Brown, C.L., Abbas, P.J., 2004. Sensitivity and specificity of averaged electrode voltage measures in cochlear implant recipients. Ear Hear. 25, 431–556.
Jasper, H.H., 1958. Report on the committee on methods of clinical examination in electroencephalography. Electroencephalogr. Clin. Neurophysiol. 10, 370–375.
Jeng, F., Abbas, P.J., Grown, C.J., Miller, C.A., Nourski, K.V., Robinson, B.K., 2008. Electrically evoked auditory steady-state responses in a guinea pig model: latency estimates and effects of stimulus parameters. Audiol. Neurotol. 13, 161–171.
Johnson, B.W., Weinberg, H., Ribary, U., Cheyne, D.O., 1988. Topographic distribution of the 40 Hz auditory evoked-related potential in normal and aged subjects. Brain Topogr. 1, 117–121.
Kang, S.Y., Colesa, D.J., Swinderski, D.L., Su, G.L., Raphael, Y., Pfingst, B., 2010. Effects of hearing preservation on psychophysical responses to cochlear implant stimulation. J. Assoc. Res. Otolaryngol. 11, 245–265.
Kreft, H.A., Donaldson, G.A., Nelson, D., 2004. Effects of pulse rate on threshold and dynamic range in Clarion cochlear-implant users. J. Acoust. Soc. Am. 115, 1885–1888.
Levi, C.E., Folsom, R.C., Dobie, R.A., 1993. Amplitude-modulated following response (AMFR): effects of modulation rate, carrier frequency, age, and state. Hear. Res. 68, 42–52.
Liégeois-Chauvel, Lorenzi, C., Trébuchon, A., Régis, J., Chauvel, P., 2004. Temporal envelope processing in the human left and right auditory cortices. Cereb. Cortex 14, 731–740.
Luke, R., Van Deun, L., Hofmann, M., van Wieringen, A., Wouters, J., 2015. Assessing temporal modulation sensitivity using electrically evoked auditory steady state responses. Hear. Res. 324, 37–45.
Luts, H., Desloovere, C., Wouters, J., 2006. Clinical application of dichotic multiple-stimulus auditory steady-state responses in high-risk newborns and young children. Audiol. Neurotol. 11, 24–37.
Lütkenhöner, B., Steinsträter, O., 1998. High-percision neuromagnetic study of the functional organization of the human auditory cortex. Audiol. Neurotol. 3, 191–213.
McKay, C.M., McDermott, H.J., 1998. Loudness perception with pulsatile electrical stimulation: the effect of interpulse intervals. J. Acoust. Soc. Am. 104, 1061–1074.
McKay, C.M., Henshall, K.R., 2010. Amplitude modulation and loudness in cochlear implantees. J. Assoc. Res. Otolaryngol. 11, 101–111.
McKay, C.M., Chandan, K., Akhoun, I., Siciliano, C., Kluk, K., 2013. Can ECAP measures be used for totally objective programming of cochlear implants. J. Assoc. Res. Otolaryngol. 14, 879–890.
Miller, C.A., Brown, C.J., Abbas, P.J., Chi, S., 2008. The clinical application of potentials evoked from the peripheral auditory system. Hear. Res. 242, 184–197.
Mühler, R., Rahne, T., Mentzel, K., Verhey, J.L., 2014. 40-Hz multiple auditory steady-state responses to narrow-band chirps in sedated and anaesthetized infants. Int. J. Pediatr. Otorhinolaryngol. 78, 762–768.
Pethe, J., Mühler, R., Siewert, K., von Specht, H., 2004. Near-threshold recordings of amplitude modulation following responses (AMFR) in children of different ages. Int. J. Audiol. 43, 339–345.
Pfingst, B.E., Xu, L., 2004. Across-site variation in detection thresholds and maximum comfortable loudness levels for cochlear implants. J. Assoc. Res. Otolaryngol. 5, 11–24.
Pfingst, B.E., Colesa, D.J., Hembrador, S., Kang, S.Y., Middlebrooks, J.C., Raphael, Y., Su, G.L., 2010. Detection of pulse trains in the electrically stimulated cochlea: effects pf cochlear health. J. Acoust. Soc. Am. 130, 245–265.
Pfingst, B.E., Zhou, N., Colesa, D.J., Watts, M.M., Strahl, S.B., Garadat, S.N., Schvartz-Leyzac, K.C., Bundenz, C.L., Raphasel, Y., Zwolan, T.A., 2015. Importance of cochlear health for implant function. Hear. Res. 322, 77–88.
Picton, T.W., Skinner, C.R., Champange, S.C., Kellet, J.C., Maiste, A.C., 1987. Potentials evoked by the sinusoidal modulation of the amplitude or frequency of a tone. J. Acoust. Soc. Am. 82, 165–178.
Picton, T.W., John, M.S., Dimitrijevic, A., Purcell, D., 2003. Human auditory steady-state responses. Int. J. Audiol. 42, 177–219.
Picton, T.W., Dimitrijevic, A., Perez-Abolo, M., Van Roon, P., 2005. Estimating audiometric thresholds using auditory steady-state responses. J. Am. Acad. Audiol. 16, 140–156.
Plomp, R., Bauman, M.A., 1959. Relation between hearing thresholds and duration for tone pulses. J. Acoust. Soc. Am. 31, 749–758.
Poulsen, C., Picton, T.W., Paus, T., 2007. Age-related changes in transient and oscillatory brain responses to auditory stimulation in healthy adults 19-45 years old. Cereb. Cortex 17, 1456–1467.
Purcell, D.W., John, S.M., Schneider, B.A., Picton, T.W., 2004. Human temporal auditory acuity as assessed by envelope following responses. J. Acoust. Soc. Am. 116, 3581–3593.
Regan, D., 1966. Some characteristics of average steady-state and transient responses evoked by modulated light. Electroenceph. Clin. Neurophysiol. 20, 238–248.
Ross, B., Borgmann, C., Draganova, R., Roberts, L.E., Pantev, C., 2000. A high-precision magentoencephalographic study of human auditory steady-state responses to amplitude-modulated tones. J. Acoust. Soc. Am. 108, 679–691.
Shannon, R.A., 1985. Threshold and loudness functions for pulsatile stimulation of cochlear implants. Hear. Res. 18, 135–143.
Shannon, R.A., 1989. A model of threshold for pulsatile electrical stimulation of cochlear implants. Hear. Res. 40, 197–204.

Shmilovitz, D., 2005. On the definition of total harmonic distortion and its effect on measurement interpretation. IEEE Trans. Power Del. 20, 526–528.
Skinner, M.W., Holden, L.K., Holden, T.A., Demorest, M.E., 2000. Effect of stimulation rate on cochlear implant recipients' thresholds and maximum acceptable loudness levels. J. Am. Acad. Audiol. 11, 203–213.
Stapells, D.R., Makeig, S., Galambos, R., 1987. Auditory steady-state responses: threshold prediction using phase coherence. Electroencephalogr. Clin. Neurophysiol. 67, 260–270.
Tlumak, A.I., Durrant, J.D., Delgado, R.E., Boston, J.R., 2011. Steady-state analysis of auditory evoked potentials over a wide range of stimulus repetition rates: profile in adults. Int. J. Audiol. 50, 448–458.
van der Beek, F.B., Briaire, J.J., Frijns, J.H.M., 2015. Population-based prediction of fitting levels for individual cochlear implant recipients. Audiol. Neurotol. 20, 1–16.
Van Maanen, A., Stapells, R.A., 2010. Multiple-ASSR thresholds in infants and young children with hearing loss. J. Am. Acad. Audiol. 21, 535–545.
Vanvooren, S., Poelmans, H., Hofmann, M., Ghesquière, P., Wouters, J., 2014. Hemispheric asymmetry in auditory processing of speech envelope modulation in prereading children. J. Neurosci. 34, 1523–1529.
Viemeister, N.F., Wakefield, G.H., 1991. Temporal integration and multiple looks. J. Acoust. Soc. Am. 90, 858–865.
Vollmer, M., Leake, P.A., Beitel, R.E., Rebscher, S.J., Snyder, R.L., 2005. Degradation of temporal resolution in the auditory midbrain after prolonged deafness is reversed by electrical stimulation of the cochlea. J. Neurophysiol. 93, 3339–3355.
Wang, Y., Ding, N., Ahmar, N., Xiang, J., Poeppel, D., Simon, J.Z., 2012. Sensitivity to temporal modulation rate and spectral bandwidth in the human auditory system: MEG Evidence. J. Neurophysiol. 107, 2033–2041.